

On The Generation of Oceanic Internal Gravity Waves by a Cyclonic Surface Stress Disturbance

Georg Sebastian Völker¹

Bruce R Sutherland²

Paul G Myers²

Maren Walter¹

¹MARUM - Center for Marine Environmental Sciences, Bremen, Germany

²Department of Earth and Atmospheric Sciences, University of Alberta, Edmonton, Canada

29th August 2016

Introduction

Model Description

Results

IW Structure and Generation Mechanisms

Energy Fluxes

Summary

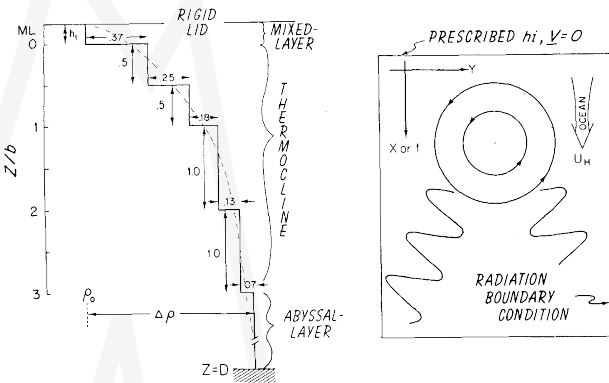


Fig. 2 from Price [1983]

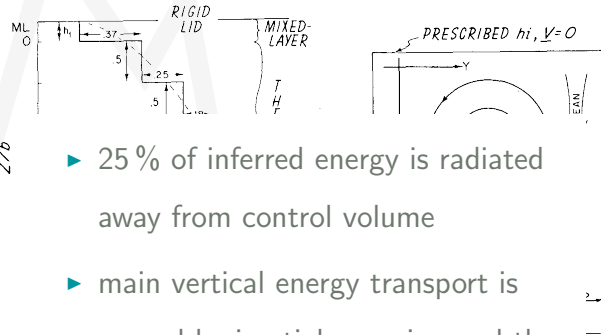
Rankine vortex with background flow;

$$R_r = 40 \text{ km}, U = 7 \frac{\text{m}}{\text{s}}$$

exponentially decaying stratification;

$$N = N_0 \exp\left(-\frac{z}{2d}\right)$$

6 vertical levels



- ▶ 25 % of inferred energy is radiated away from control volume
- ▶ main vertical energy transport is caused by inertial pumping and the corresponding pressure field

Rankine vortex with background flow;

$$R_r = 40 \text{ km}, U = 7 \frac{\text{m}}{\text{s}}$$

exponentially decaying stratification;

$$N = N_0 \exp\left(-\frac{z}{2d}\right)$$

6 vertical levels

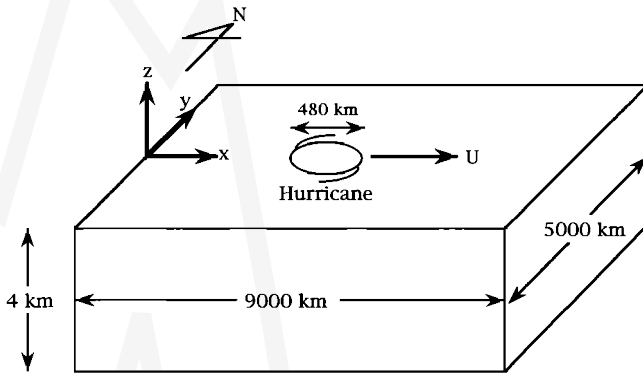


Fig. 1 from Niwa and Hibiya [1997]

Rankine vortex moving
across domain;

$$R_r = 40 \text{ km}, U = 5 \frac{\text{m}}{\text{s}}$$

constant stratification;

$$N = 0.5 \cdot 10^{-2} \frac{\text{rad}}{\text{s}}$$

40 vertical levels



4 kn

- ▶ energy transport is caused by inertial internal waves
- ▶ non-linear triad interactions generate superharmonics with frequencies $2f$ and $3f$ and low vertical wave numbers



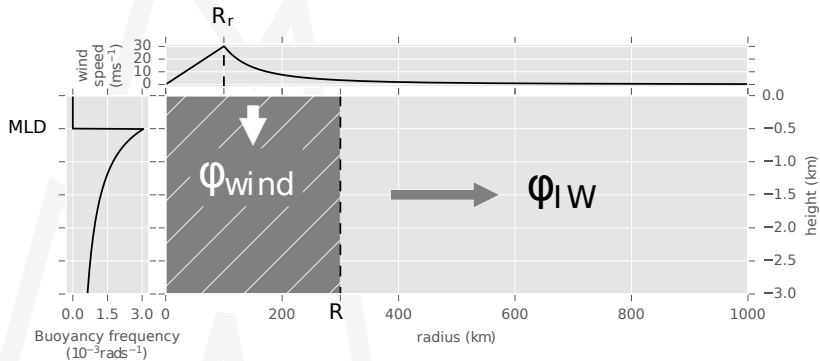
Rankine vortex moving across domain;

$$R_r = 40 \text{ km}, U = 5 \frac{\text{m}}{\text{s}}$$

constant stratification;

$$N = 0.5 \cdot 10^{-2} \frac{\text{rad}}{\text{s}}$$

40 vertical levels



$$dr = 976.56 \text{ m}$$

$$dz = 23.44 \text{ m}$$

$$dt = 18 \text{ s}$$

$$\nu_r = 1 \frac{\text{m}^2}{\text{s}}$$

$$R_{max} = 1000 \text{ km}$$

$$z_{min} = 3000 \text{ m}$$

$$t_{end} = 40 \text{ d}$$

$$\nu_z = 0.03 \frac{\text{m}^2}{\text{s}}$$

based on Mcmillan and Sutherland [2010]
and Holdsworth and Sutherland [2013]

$$\partial_t \omega = -ru\partial_r \left(\frac{\omega}{r} \right) - w\partial_z \omega + \partial_z \left(\frac{v^2}{r} + fv \right) + D_\nu(\omega)$$

$$\partial_t v = -u\partial_r v - w\partial_z v - \frac{uv}{r} - fu + D_\nu(v)$$

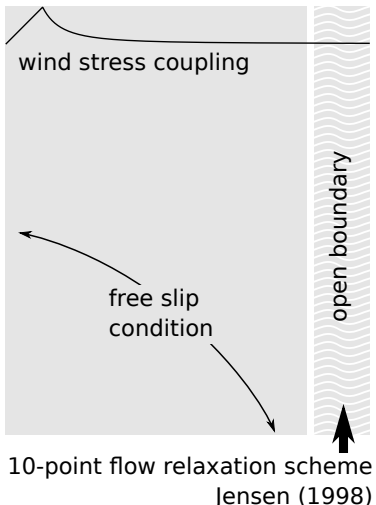
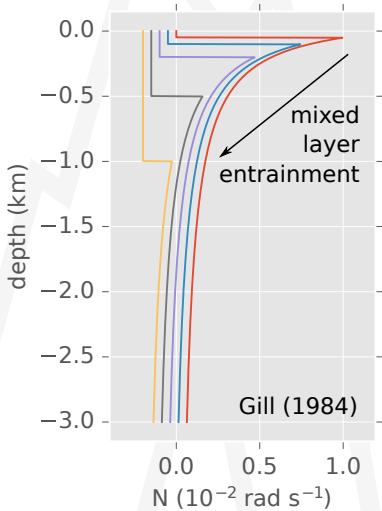
$$\partial_t \rho' = -u\partial_r \rho' - w\partial_z \rho' - w\partial_z \bar{\rho} + D_\kappa(\rho')$$

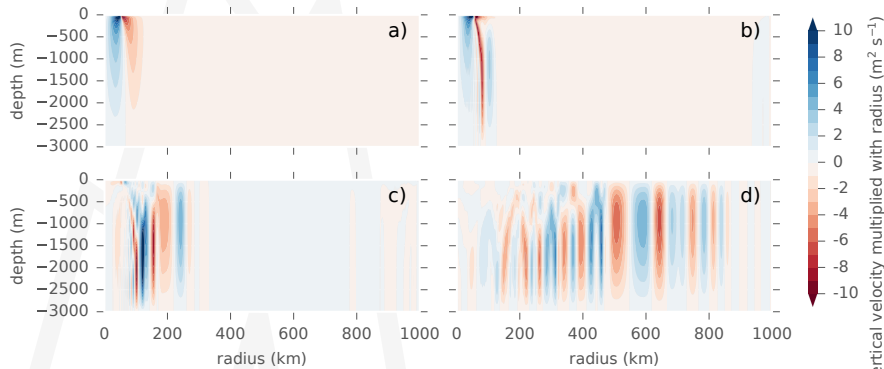
$$\Delta_r \psi = \frac{\psi}{r^2} - \omega$$

notation:

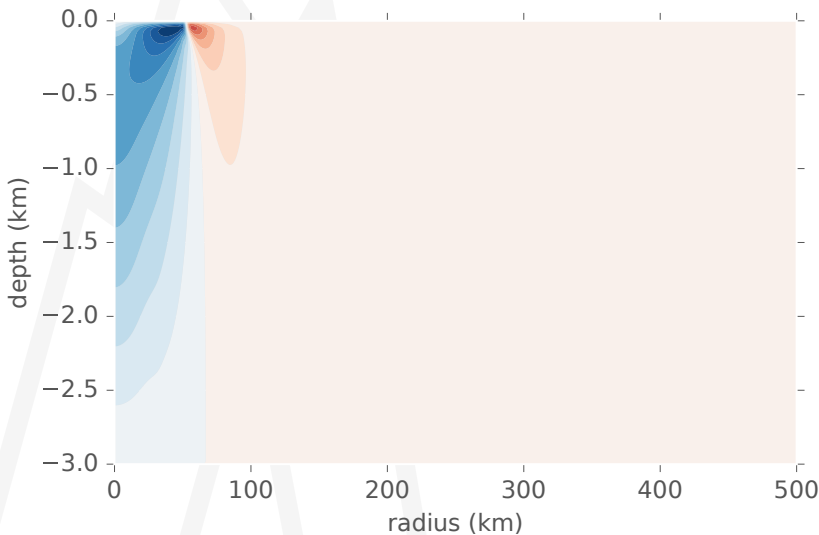
$$u = u_r \qquad w = u_z$$

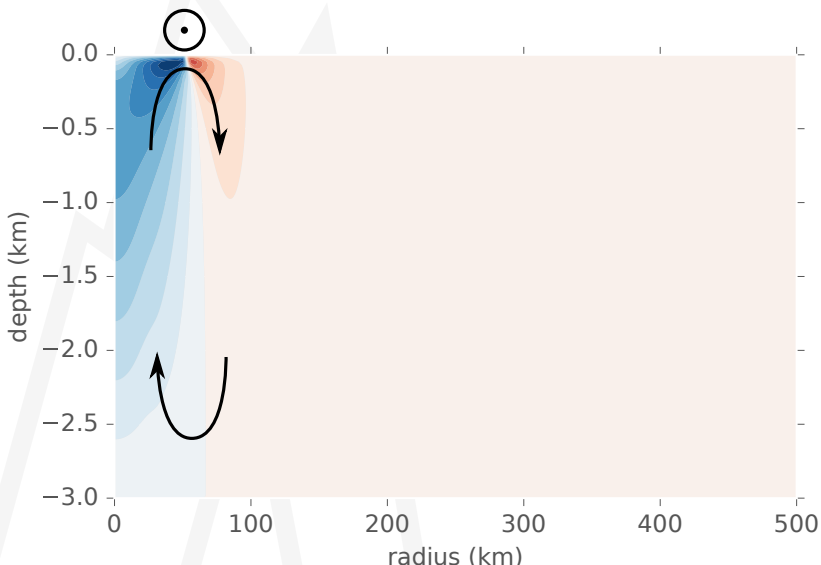
$$v = u_\theta \qquad \omega = \partial_z u - \partial_r w$$

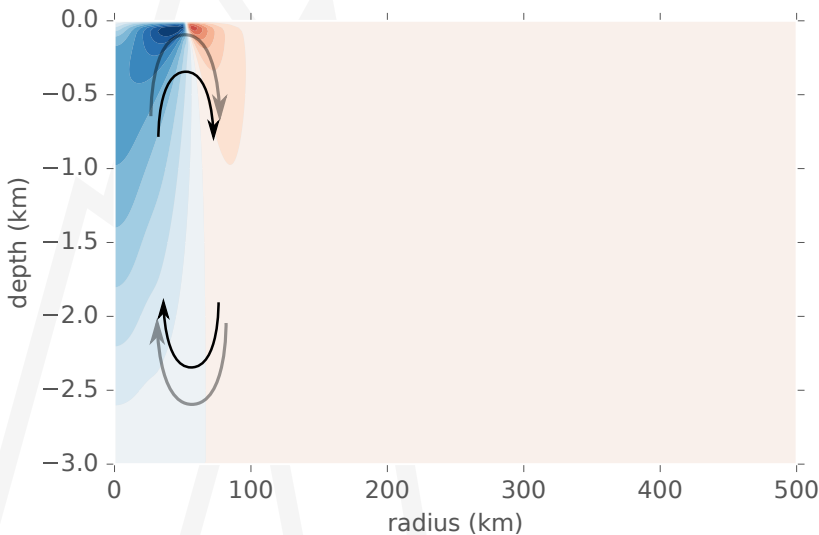


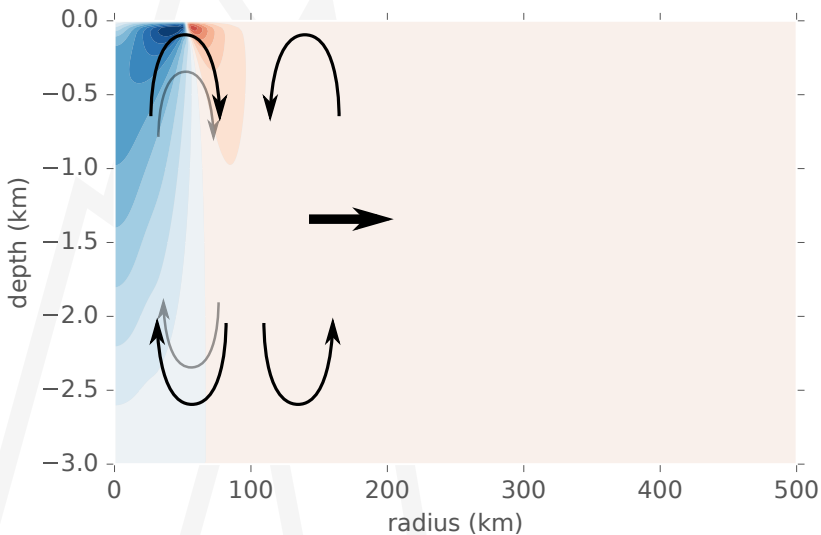


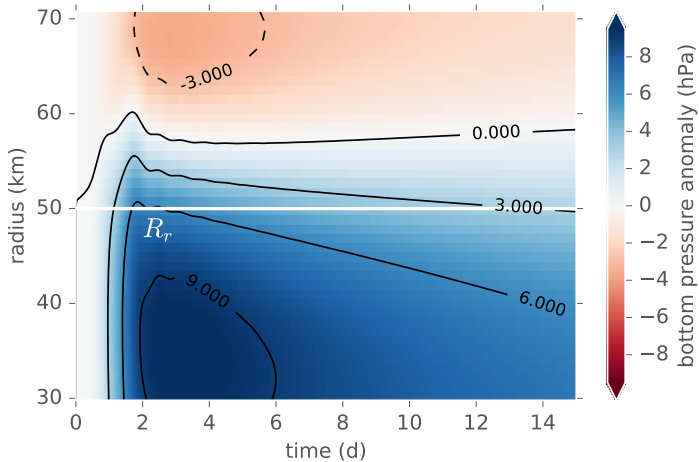
Snapshots of vertical velocity for the control run at model time a) 12h b) 22.5h c) 50h and d) 150h. For scaling reasons the vertical velocity was multiplied by the radius.



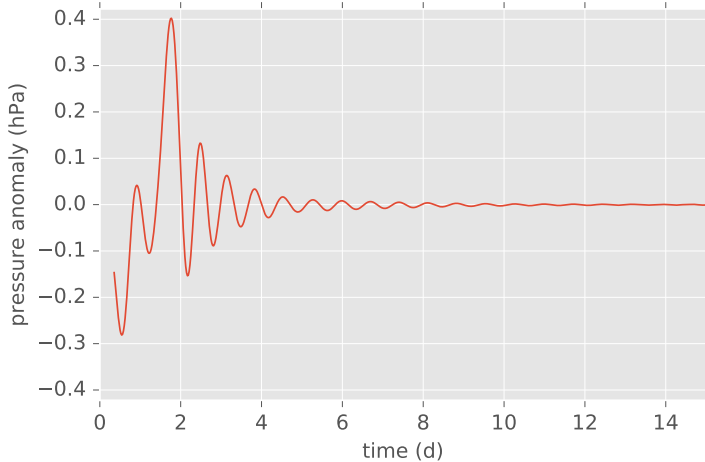




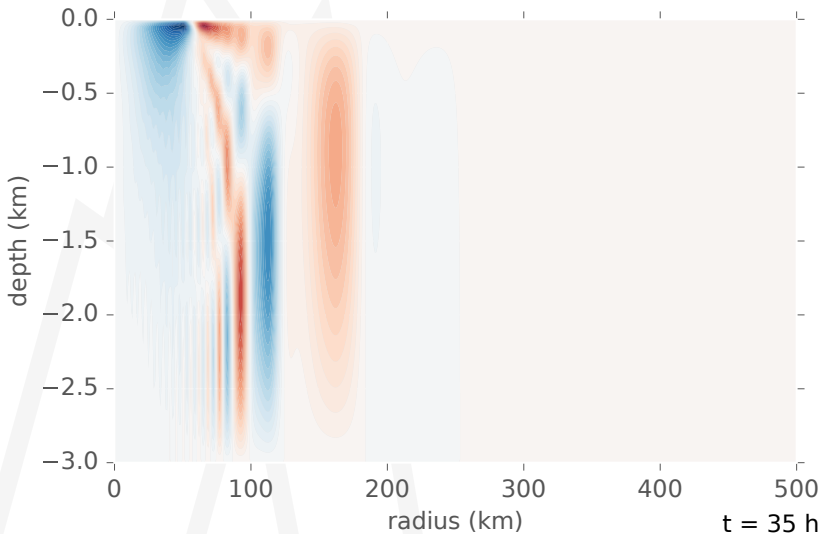




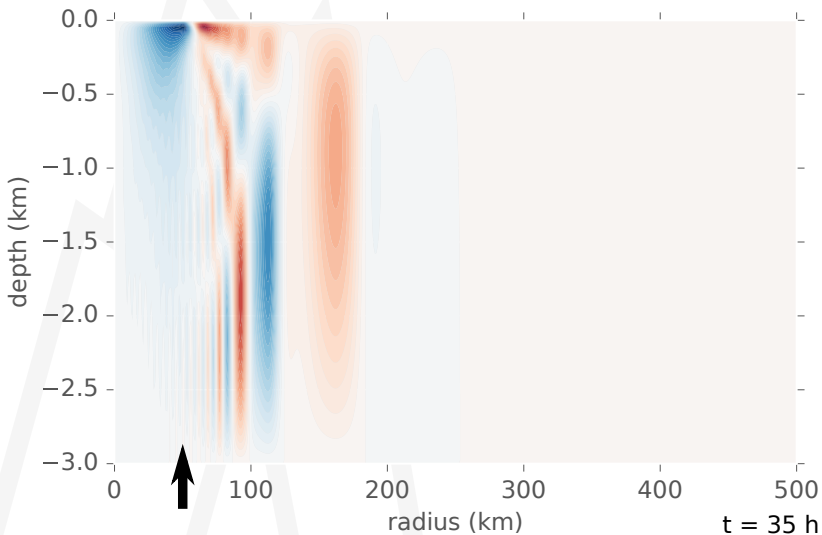
Bottom pressure in early stages of the control run close to the critical radius R_r .

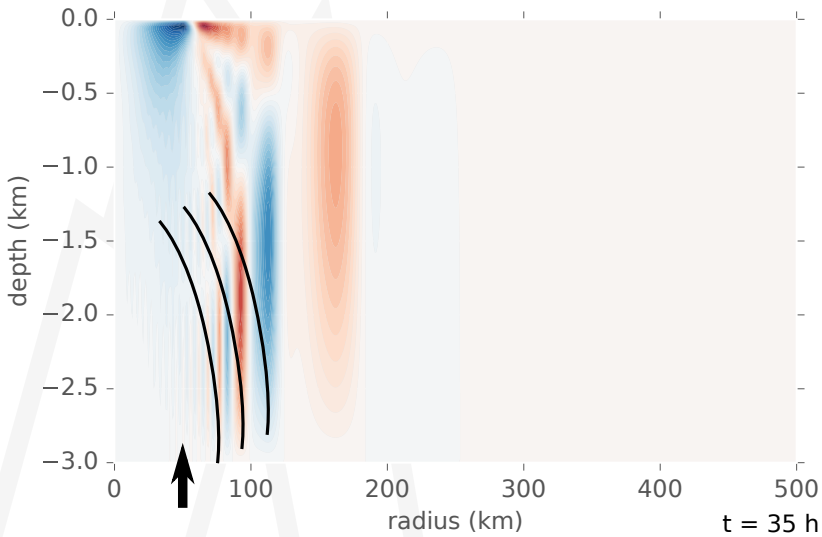


Time series of the bottom pressure at the critical radius R_r .

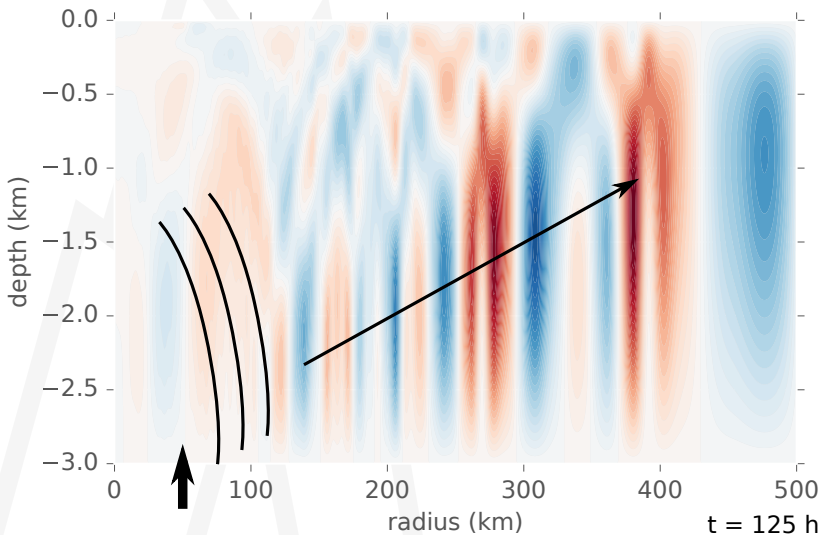


Snapshot of vertical velocity at indicated time.

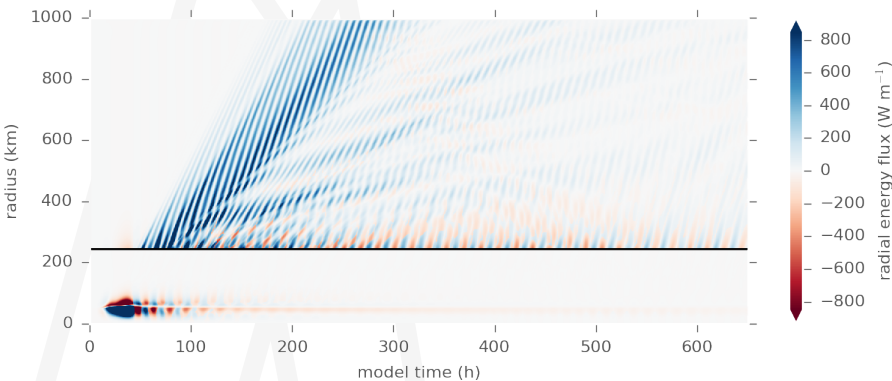




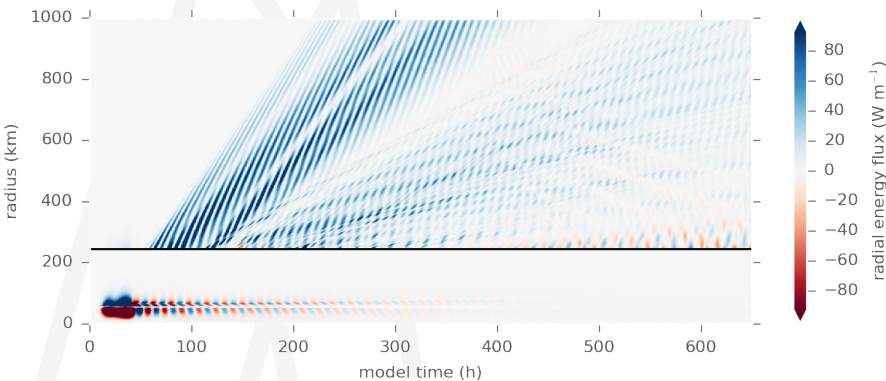
Generation of higher modes through
pressure oscillation.



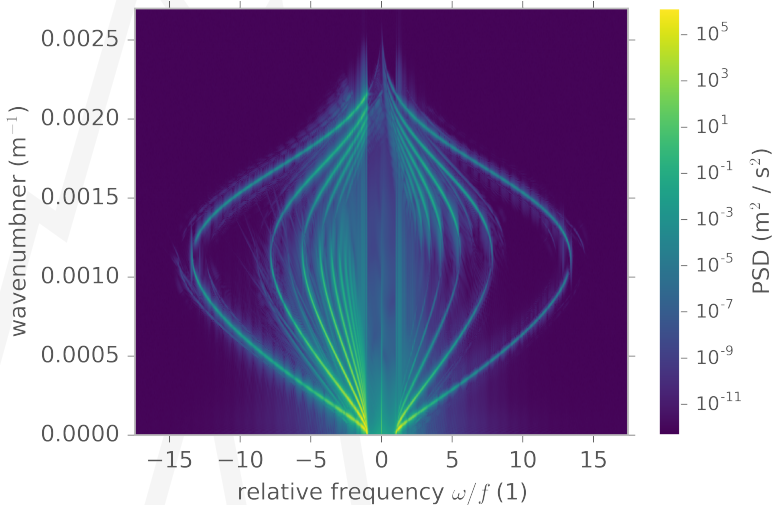
Upward radiation of higher modes.



Hovmoeller plot of the radial energy flux $2\pi r u' p'$ as a function of time and radius for control run. The maximal value in depth is shown.

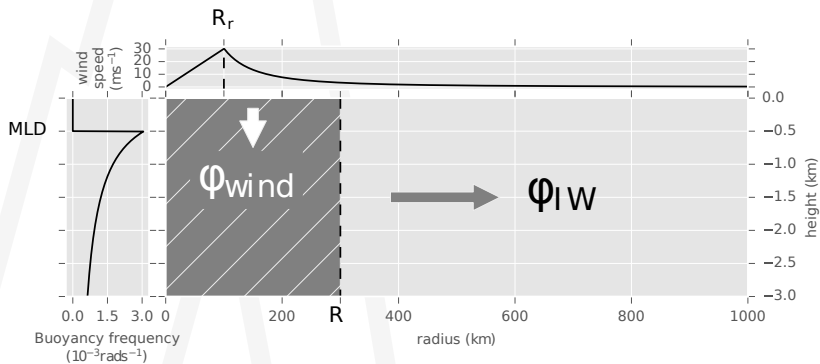


Same as before but with $MLD = 500 \text{ m}$. The radiated wave packets have lower radial wavenumbers and group velocities.

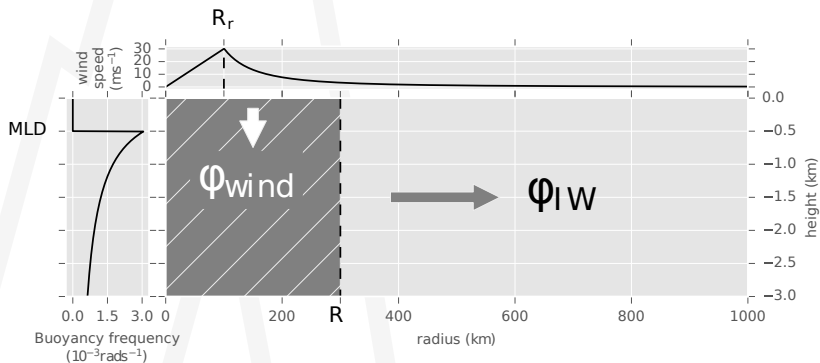


Vertical wavenumber - frequency spectrum of vertical velocity. Spectrum is averaged in depth.

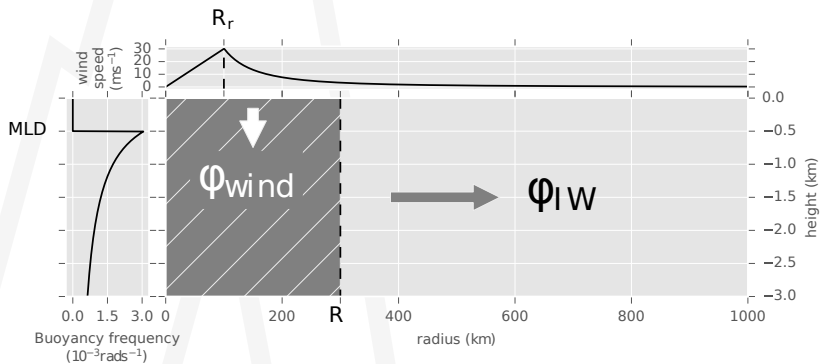
$$0 = \Phi_{wind} - E_v + (\Phi_{IW} + D)$$



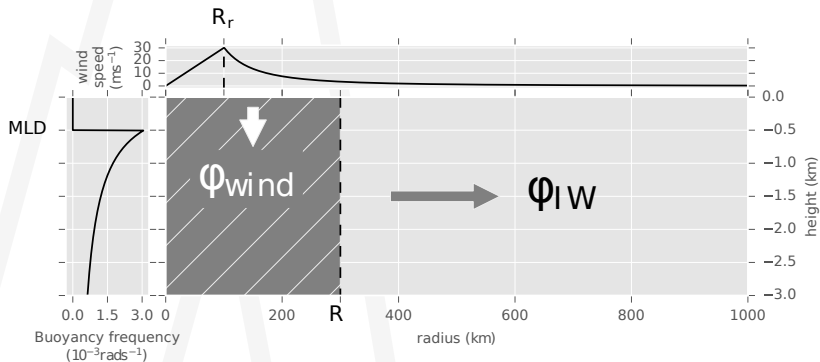
$$\Phi_{wind} = \iiint \tau \cdot \mathbf{u} \, r d\theta dr dt$$

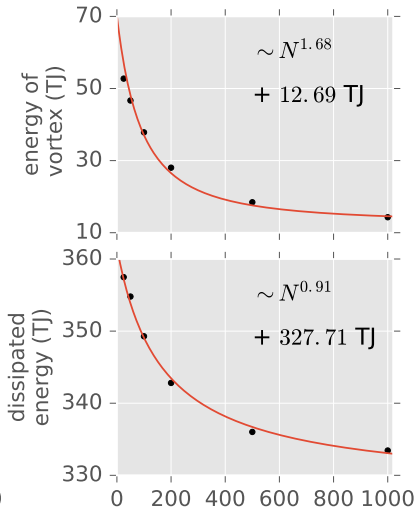
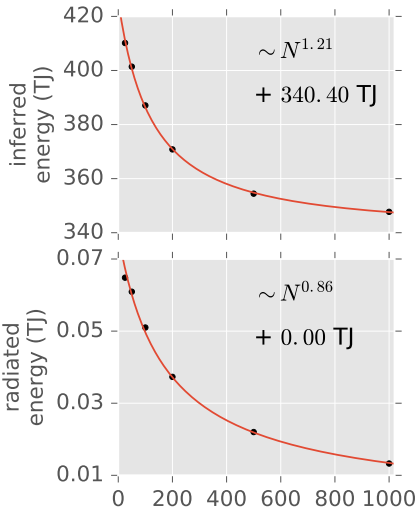


$$\Phi_{IW} = \iint u' p' R d\theta dz$$



$$E_v = \left[\iiint (\mathcal{E}_{kin} + \mathcal{E}_{APE}) r d\theta dr dz \right]_{t=T}$$



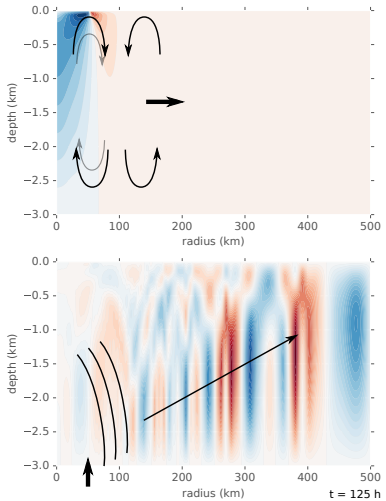


MLD (m)	ϕ_{wind} (TJ)	E_v/ϕ_{wind} (%)	ϕ_{IW}/ϕ_{wind} (%)	D/ϕ_{wind} (%)
25	410.16	12.86	-0.0158	-87.12
50	401.41	11.63	-0.0152	-88.36
100	387.07	9.78	-0.0132	-90.21
200	370.81	7.56	-0.0101	-92.43
500	354.44	5.20	-0.0062	-94.79
1000	347.72	4.11	-0.0038	-95.89
3000	340.40	3.73	0.0000	-96.27

- ▶ assume $\sim 10^3$ storms a year [Condron and Renfrew, 2012]

ϕ_{wind} (GW)	11.03 – 13.01
D (GW)	10.57 – 11.34
ϕ_{IW} (MW)	0.42 – 2.06

- ▶ two generation mechanisms
 - ▶ periodic inertial pumping
 - ▶ oscillating bottom intensified pressure field
- ▶ energetics
 - ▶ wind power: 11.03 – 13.01 GW
 - ▶ IW flux: 0.42 – 2.06 MW
 - ▶ most IWs are radiated due to the movement of a storm



Condron, A., and I. a. Renfrew, 2012: The impact of polar mesoscale storms on northeast Atlantic Ocean circulation. *Nat. Geosci.*, **6** (1), 34–37, doi:10.1038/ngeo1661.

Gill, A. E., 1984: On the Behavior of Internal Waves in the Wakes of Storms. *J. Phys. Oceanogr.*, **14** (7), 1129–1151, doi:10.1175/1520-0485(1984)014<1129:OTBOIW>2.0.CO;2.

Holdsworth, A. M., and B. R. Sutherland, 2013: Influence of lock aspect ratio upon the evolution of an axisymmetric intrusion. *J. Fluid Mech.*, **735**, 1–11, doi:10.1017/jfm.2013.517.

Jensen, T. G., 1998: Open boundary conditions in stratified ocean models. *J. Mar. Syst.*, **16** (3-4), 297–322.

Kang, D., and O. Fringer, 2010: On the Calculation of Available Potential Energy in Internal Wave Fields. *J. Phys. Oceanogr.*, **40** (11), 2539–2545, doi:10.1175/2010JPO4497.1.

Mcmillan, J. M., and B. R. Sutherland, 2010: The lifecycle of axisymmetric internal solitary waves. *Nonlinear Process. Geophys.*, **17** (2010), 443–453, doi:10.5194/npg-17-443-2010.

Niwa, Y., and T. Hibiya, 1997: Nonlinear processes of energy transfer from traveling hurricanes to the deep ocean internal wave field. *J. Geo.*, **102** (C6), 12,464–12,477.

Price, J. F., 1983: Internal Wave Wake of a Moving Storm. Part I. Scales, Energy Budget and Observations. 949–965 pp., doi:10.1175/1520-0485(1983)013<0949:IWWOAM>2.0.CO;2.

APPENDIX I

Dissipation Operators

Wind Stress

Parametrization

Surface Velocities

$$D_\nu(x) = \nu_r \left(\frac{1}{r} \frac{\partial}{\partial r} \left(r \frac{\partial x}{\partial r} \right) - \frac{x}{r^2} \right) + \nu_z \frac{\partial^2 x}{\partial z^2}$$

$$D_\kappa(x) = \kappa_r \frac{1}{r} \frac{\partial}{\partial r} \left(r \frac{\partial x}{\partial r} \right) + \kappa_z \frac{\partial^2 x}{\partial z^2}$$

$$\tau_r = \frac{\partial u}{\partial z} = \rho_{air} C_d (u_{10} - u_{surface})^2$$

$$\tau_\theta = \frac{\partial v}{\partial z} = \rho_{air} C_d (v_{10} - v_{surface})^2$$

$$u_{surface} = \frac{\Delta z}{2\nu_z \rho_0} \tau_r + u_n$$

$$v_{surface} = \frac{\Delta z}{2\nu_z \rho_0} \tau_\theta + v_n$$

APPENDIX II

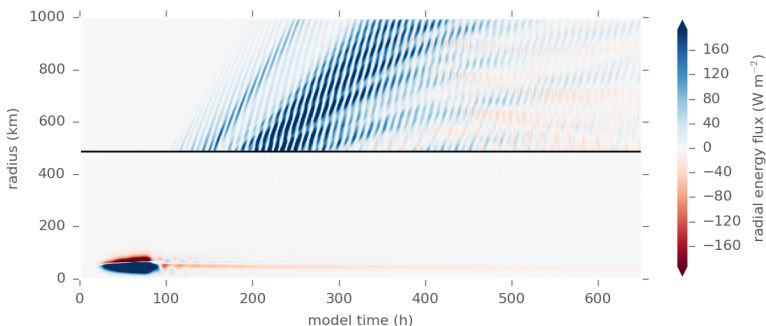
APE following Kang and Fringer [2010]

$$\mathcal{E}_{kin} = \frac{\rho_0}{2} (u^2 + v^2 + w^2)$$
$$\mathcal{E}_{APE} \approx \frac{g^2 \rho'^2}{2 \rho_0 N^2} + \frac{g^3 \partial_z(N^2) \rho'^3}{6 \rho_0^2 N^6}$$

APPENDIX III

Long Pulse

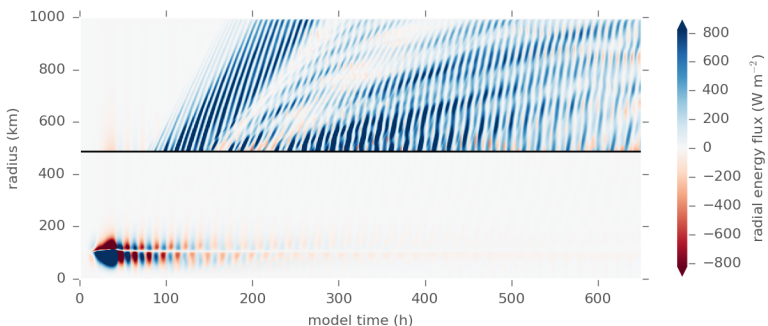
- ▶ longer forcing time scale
- ▶ reduced inertial pumping
- ▶ very much reduced low mode radiation



APPENDIX III

Double Radius

- ▶ increase in both spacial scales
- ▶ depth smaller relative to vertical scale
- ▶ more dominant higher modes



APPENDIX III

Double Wind Speed

- ▶ very similar structure
- ▶ very much increased radiation
- ▶ meaning of singular strong storms?

